Structural connectome changes in episodic migraine: the role of the cerebellum

Ana Matoso MSc[1], Ana R Fouto PhD[1], Inês Esteves MSc[1], Amparo Ruiz-Tagle MSc[1], Gina Caetano PhD[1], Nuno A da Silva PhD[2], Pedro Vilela MD[3], Raquel Gil-Gouveia MD[4,5], Rita G Nunes PhD[1], and Patricia Figueiredo DPhil[1]

[1]Institute for Systems and Robotics – Lisboa and Department of Bioengineering, Instituto Superior Técnico, University of Lisbon, Portugal

[2]Learning Health, Hospital da Luz, Lisbon, Portugal

[3]Imaging Department, Hospital da Luz, Lisbon, Portugal

[4]Neurology Department, Hospital da Luz, Lisbon, Portugal

[5]Center for Interdisciplinary Research in Health, Universidade Católica Portuguesa, Lisbon, Portugal

Corresponding Author:

Ana Matoso, Institute for Systems and Robotics – Lisboa and Department of Bioengineering, Instituto Superior Técnico, University of Lisbon, Portugal.

Avenida Rovisco Pais 1, 1049-001

Email: anamatoso@tecnico.ulisboa.pt

ABSTRACT

Background: Migraine's pathophysiology remains poorly understood, yet a growing number of studies have shown structural connectivity disruptions across large-scale brain networks. Both macro- and micro-structural changes have been found in the cerebellum of migraine patients; however, the cerebellum has not been considered in previous structural connectivity studies in migraine.

Purpose: To comprehensively explore the structural connectivity of the entire brain, including the cerebellum, in individuals diagnosed with episodic migraine without aura during the interictal phase, compared with healthy controls.

Study Type: Retrospective

Population: 14 migraine patients and 15 healthy controls, all female.

Field Strength/Sequence: 3 Tesla, diffusion-weighted imaging (multi-shell) and T1-weighted MPRAGE.

Assessment: A whole-brain parcellation was performed, including cortical and subcortical regions and the cerebellum, by employing two different atlases, and the structural connectome was estimated based on diffusion MRI.

Connectivity patterns, global and local graph metrics, and the number of reconstructed streamlines were compared between patients and controls.

Statistical Tests: Network-Based Statistics toolbox, and Wilcoxon Rank-Sum Test. A p-value of 0.5 was considered significant (in the case of nodal metrics, corrected using the Bonferroni correction).

Results: We found increased structural connectivity in migraine patients relative to healthy controls with a distinct involvement of cerebellar regions, using both parcellations ($p<0.03$ for both). Specifically, the node degree of the posterior lobe of the cerebellum was greater in patients than in controls ($p<0.05$) and patients presented a higher number of streamlines within the anterior limb of the internal capsule ($p<0.5$). Moreover, the connectomes of patients exhibited greater global efficiency ($p<0.05$) and shorter characteristic path length ($p<0.01$), which correlated with the disease duration (Pearson $r=0.56$, $p=0.038$).

Data conclusion: Migraine patients show increased integration within structural brain networks and underscore the significance of the cerebellum in migraine.

Keywords: Migraine, MRI, Structural Connectivity, Cerebellum, Tractography

1. INTRODUCTION

About 17% of people suffer from migraine, making it one of the most prevalent neurological diseases worldwide (1). Although its pathophysiology is still not fully understood, multiple studies have found structural and functional abnormalities throughout extensive brain networks (2-10). Several studies have reported structural connectivity (white matter) alterations in migraine (3–7) based on diffusion Magnetic Resonance Imaging (dMRI).

Some studies found increased connectivity between cortical regions involved in pain perception and processing (3), and between subcortical regions such as the thalamus and the caudate nucleus (4), suggesting that subcortical networks are strengthened in migraine (4, 5). Other studies investigated connectome differences from a graph theory perspective using the connectivity between regions as edges and the regions as nodes. Li et. al. (6) found a decreased characteristic path length in migraine patients, which points to an increased number of short-distance connections and hence an increased integration. Specifically, increased efficiency (integration measure) in the putamen, pallidum, and thalamus was found, which is indicative of increased information transfer in these regions. Furthermore, altered node centrality was found in subcortical regions such as the thalamus, the parahippocampal gyrus, and the anterior cingulate gyrus (8).

Concerning structural alterations, Mehnert et al. (11) reported gray matter volume changes in the cerebellum in migraine patients, especially in the crus, and Qin et al. (12) found changes in FA in the vermis and the bilateral lobules. Additionally, existing evidence suggests that migraine patients are more prone to ischaemic lesions in the posterior lobe of the cerebellum (13).

Critically, although the cerebellum has an important role in pain processing (14), to our knowledge no study of structural connectivity using tractography in migraine has included it.

Moreover, despite the accumulation of evidence supporting structural connectivity alterations in migraine, previous studies either focused entirely on chronic migraine, combined the chronic and episodic forms of migraine, or mixed patients with and without aura (3, 4, 10). Indeed it is anticipated that patients with chronic migraine will present

more complex brain changes than those with lower frequency of attacks and fewer comorbidities. On the other hand, the aura, experienced by a small subset of migraine patients, is known to be associated with very specific phenomenology and distinct pathophysiological processes (1). The episodic migraine without aura cohort is by far the most prevalent.

In our study, we aimed to investigate structural connectivity changes in patients with episodic migraine without aura, considering the whole brain including cortical and subcortical regions as well as the cerebellum.

2. METHODS

An overview of the methods pipeline can be seen in Figure 1.

2.1. Participants

This study analyzed data from a cohort comprised of 14 adult females, aged 18 to 55 years old, with episodic migraine without aura diagnosed according to the criteria of the 3rd edition of the International Classification of Headache Disorders (ICHD-III) (15). These participants are otherwise healthy, without any diagnosed condition significantly hindering active and productive life, and with a life expectancy exceeding 5 years. None was receiving treatment with psychoactive drugs, including anxiolytics, antidepressants, anti-epileptics, and any migraine prophylactics. Imaging data was acquired during the post-ovulation period, corresponding to the interictal phase, as participants in the cohort experienced menstrual-related migraine attacks. Prior to scanning, participants were required to be free from pain for at least 48 hours, with confirmation of the absence of a migraine attack obtained 72 hours post-scan. Healthy controls were matched for gender, age, contraceptive use, and menstrual phase at the time of scanning. All participants provided written informed consent and the study was carried out following the Declaration of Helsinki upon approval by the local Ethics Committee.

The following demographic and clinical parameters were collected (Table 1): age (years), frequency (migraine attacks per month), age of onset of migraine (years), and disease duration (years).

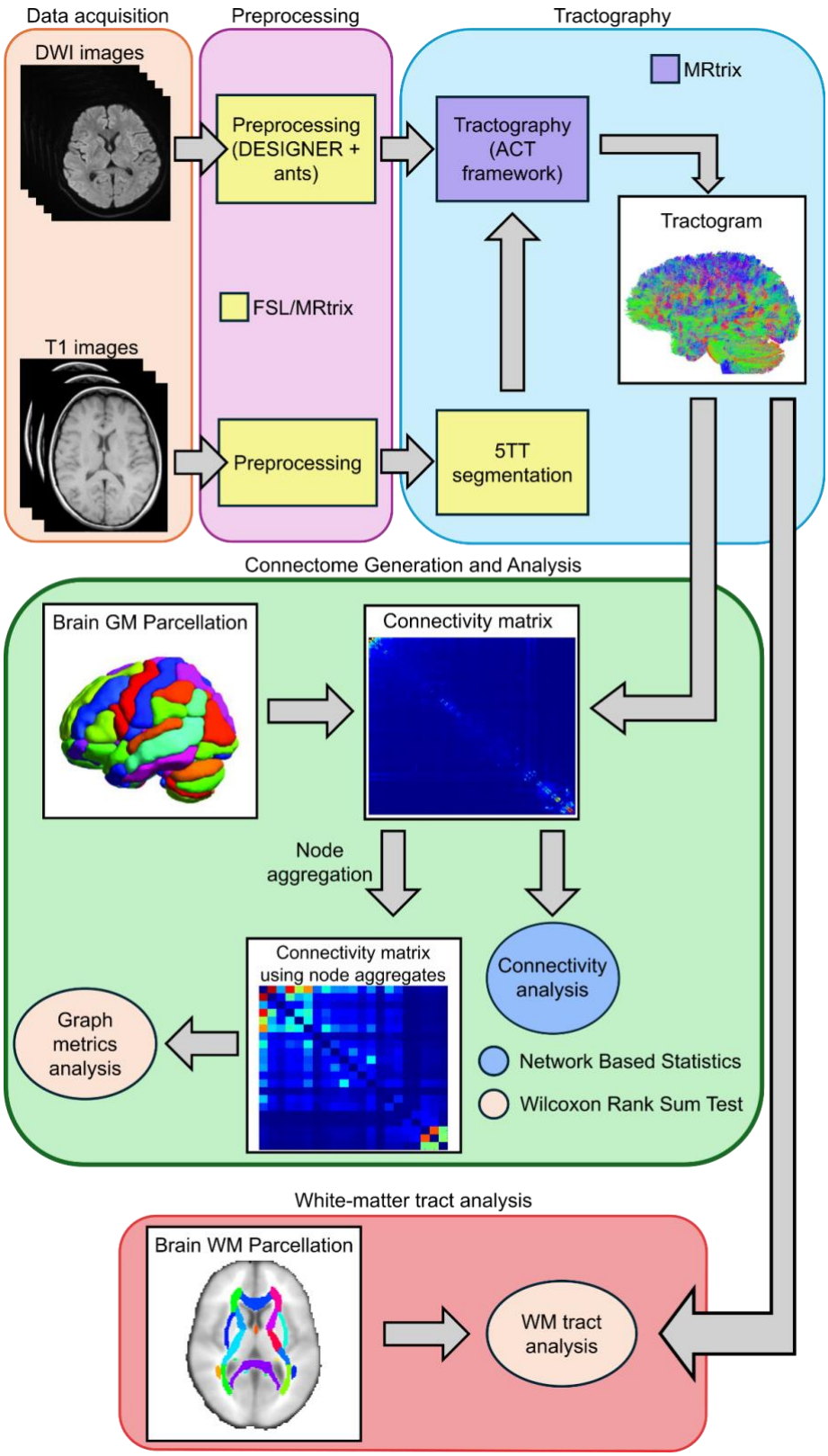

Figure 1: Overview of the data processing pipeline, from the acquisition of the images to the connectome generation, including the different analyses performed.

Table 1: Clinical and demographic characteristics of migraine patients (M) and healthy controls (HC). No significant changes were found between patients and controls concerning their age (p=0.08). †Mann-Whitney U test.

Parameter	Group	Mean ± SD	P-value
Age (years)	M	35.5 ± 8.7	0.08†
	HC	30.8 ± 6.8	
Frequency (migraine attacks/month)	M	2.4 ± 1.9	-
Age Onset (Years)	M	15.7 ± 7.3	-
Pain Intensity (0-10)	M	6.62 ± 1.31	-
Disease Duration (Years)	M	20.1 ± 11.0	-

2.2. Data Acquisition

The MRI data was acquired using a 3 Tesla system (Siemens Vida), equipped with a 64-channel receiver head coil. Regarding the dMRI data, an echo planar imaging sequence was used with the following parameters: TR = 6800 ms, TE = 89 ms, 66 slices, and 2 mm isotropic voxel size with Field-of-view (FOV) = 110 x 110 x 66. The sampling scheme consisted of 3 diffusion shells (multi-shell) with b = 400, 1000, 2000 s/mm2 along 32, 32, 60 gradient directions, respectively, and 8 non-diffusion-weighted volumes (b=0). Structural T1-weighted images were also acquired with a 3D magnetization-prepared rapid gradient echo (MPRAGE) sequence with the following parameters: 1mm isotropic voxel size, TR = 2300 ms, TE = 2.98 ms, TI = 900 ms, FOV = 256 × 240 × 128 mm3.

2.3. Data Preprocessing

Image processing was then conducted using a combination of FSL (16) (fsl.fmrib.ox.ac.uk) and MRtrix (17) (www.mrtrix.org) tools. The following preprocessing procedures were applied to the dMRI data based on the DESIGNER (Diffusion parameter EStImation with Gibbs and NoisE Removal) pipeline (18): denoising, Gibbs ringing correction, and Rician bias correction were performed with MRtrix, followed by geometric and eddy-current distortions and motion correction with FSL. After this, bias field correction was done with MRtrix using the *ants* option.

2.4. Tractography

To calculate the streamlines (tracts) of white matter fibers, MRtrix was used. Firstly, the basis functions for each tissue type were estimated from the subject's dMRI data. Then, the fiber orientation density functions (FODf) were calculated using multi-shell multi-tissue constrained spherical deconvolution (19) followed by their normalization to enable the comparison between subjects. Afterwards, Anatomically-Constrained Tractography (20) was performed which makes use of prior anatomical knowledge to restrict the generated streamlines by, for instance, preventing streamlines from ending in implausible places such as in the middle of white matter or in the cerebrospinal fluid. Then, a seed region along the boundary between gray matter and white matter was created from which seed points were randomly generated. From these points, the streamlines were reconstructed thus creating a tractogram. Ten million streamlines were seeded with a maximum length of 25 cm. Subsequently, spherical deconvolution-informed filtering of tractograms (SIFT) (21) was performed. Finally, the tractogram was utilized to determine the connectivity between different regions of interest (ROI) and to generate a connectome.

2.5. Connectome generation

Two sets of ROIs covering the whole brain were defined using two different parcellations: i) *Schaefer + SC + CB parcellation:* 100 cortical regions from the Schaefer atlas (22) combined with 12 subcortical regions (SC) and 26 cerebellum (CB) regions

from the Automated Anatomical Labeling atlas with 116 nodes (AAL116) (23); and ii) *AAL116 parcellation:* the 116 regions of the AAL116 atlas, which includes cortical regions as well as the same SC and CB regions as in i).

For each of these parcellations, a connectivity matrix was calculated based on the streamlines that connect each pair of ROIs and the volumes of those ROIs, according to:

$$a_{ij} = \frac{2}{V_i + V_j} n_{ij} \quad (1)$$

where a_{ij} is the entry of the connectivity matrix concerning ROI *i* and ROI *j*, n_{ij} is the number of streamlines between the two ROIs given by the tractogram, and V_i and V_j are the volumes of ROI *i* and ROI j, respectively. Note that, due to the absence of directionality in dMRI, the connectivity matrix is symmetric. Also, self-connections (streamlines that begin and end in the same ROI) were not considered, and as such the connectivity matrix has a zero diagonal.

2.6. Connectome Analysis

2.6.1. Connectivity Analysis

To detect significant connectivity changes between patients and controls, the network-based statistics toolbox (NBS) (24) was used. This toolbox leverages permutation testing to assess the statistical significance across subnetworks of connections. A threshold of 3.1 was applied and 5000 permutations were used to generate the empirical null distribution for the size of the largest connected component (subnetwork). Components whose size exceeded the family-wise error rate (FWER) corrected p-value of 0.05 were considered statistically significant.

For a more straightforward interpretation of the results, the regions (nodes) of each parcellation were grouped into larger regions (node aggregates) according to the larger-scale organization of each atlas: i) *Schaefer + SC + CB parcellation:* the 7 canonical resting-state functional networks identified by Yeo (25) + subcortical regions + crus + posterior lobe of the cerebellum (PLC) + vermis; and ii) *AAL116 parcellation*: 4 lobes (occipital, parietal, frontal and temporal) + subcortical regions + crus + PLC + vermis. For all regions but the vermis, left and right regions were considered separately.

2.6.2. Graph Metrics Analysis

The following graph metrics were calculated on the node aggregates described above using the Brain Connectivity Toolbox (26): global metrics (characteristic path length, global efficiency, average degree, clustering coefficient, and small-worldness) and a local metric (node degree). For the comparisons between patients and controls, a Wilcoxon Rank Sum Test was used. The correlation between the graph metrics and the clinical parameters was calculated using the Pearson correlation coefficient, where a threshold p-value of 0.05 was considered significant. For both the group comparisons and the correlations, a p-value of 0.05 was considered significant for the global metrics, whilst a p-value of 0.05 corrected for the number of nodes using Bonferroni correction was considered significant for the nodal metrics ($p<0.0024$ and $p<0.0033$, for the *Schaefer + SC + CB parcellation* and *AAL116 parcellation*, respectively).

2.6.3. White Matter Tract Analysis

Additionally, using the tractogram of each subject, the number of reconstructed streamlines was computed within each ROI of a white matter atlas (ICBM-DTI-81 white-matter labels atlas (27)). A Wilcoxon Rank Sum Test was used to compare the number of reconstructed streamlines in each ROI between groups. For this test, a p-value of 0.05 was considered significant (uncorrected for multiple comparisons across ROIs).

3. RESULTS

No significant changes were found between patients and controls concerning their age ($p=0.08$).

An example of a tractogram and the corresponding connectivity matrices, obtained from a representative patient with each parcellation, are shown in Figure S1 of the supplementary material.

3.1. Connectivity Analysis

Several connections exhibited significantly increased connectivity in patients relative to controls, for both parcellations (listed in Table S1 and Table S2 in the Supplementary Material). Specifically, a network of increased connectivity in patients was found in both parcellations with p=0.027 for the Schaefer+SC+CB parcellation and p=0.009 for the AAL116 parcellation

For the visualization of significant connectome differences, we display the total number of connections exhibiting significant differences between patients and controls within each node aggregate in Figure 2, both for the Schaefer + SC + CB parcellation (left) and the AAL116 parcellation (right).

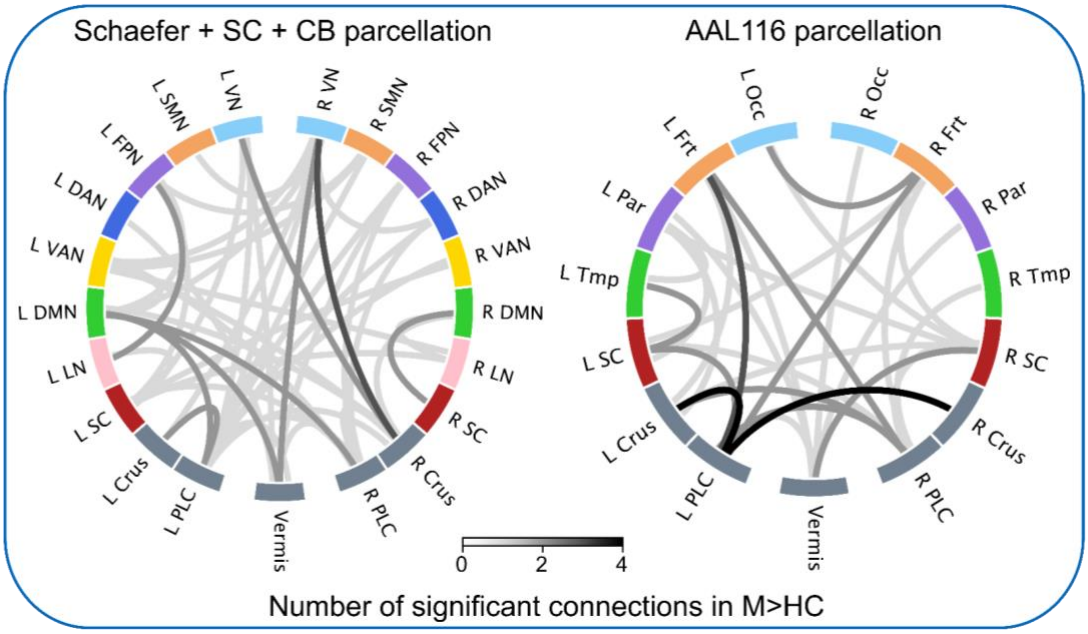

Figure 2: Connectograms of connections exhibiting significantly increased connectivity in patients (M) vs. controls (HC), detected by NBS using both the Schaefer + SC + CB parcellation (M>HC, p=0.027) and the AAL116 parcellation (M>HC, p=0.009). The edges represent the sum of connections with significant differences within each region (node aggregate). L=Left, R=Right, VN=Visual Network, SMN=Somatossensory Network, FPN=Fronto-Parietal Network, DAN=Dorsal Attention Network, VAN=Ventral Attention Network, DMN=Default Mode Network, LN=Limbic Network, Occ=Occipital, Frt=Frontal, Par=Parietal, Tmp=Temporal, SC=Subcortical PLC=Posterior Lobe of the Cerebellum.

Despite some differences between the results obtained with the two parcellations, common changes in connectivity patterns exist. Specifically, increased connectivity in patients was consistently observed with both parcellations between the left crus and the left posterior lobe of the cerebellum, as well as between the occipital lobe/visual network and the vermis. Additionally, increased connectivity was also evident between various cerebellar regions and frontal and parietal regions. In summary, a distinctive pattern of increased cerebellar connectivity was consistently observed in patients relative to controls, using both parcellations.

3.2. Graph Metrics Analysis

Concerning local graph metrics, the only significant between-groups difference was found in the node degree of the right and left posterior lobe of the cerebellum, which is increased in patients relative to controls using both parcellations, as shown in Figure 3. The results for the global graph metrics are presented in Figure 4. A significant decrease of the characteristic path length and a significant increase of the global efficiency were observed in patients relative to controls. The average degree and the clustering coefficient only showed significant between-group differences when using the AAL116 parcellation, both being higher in patients.

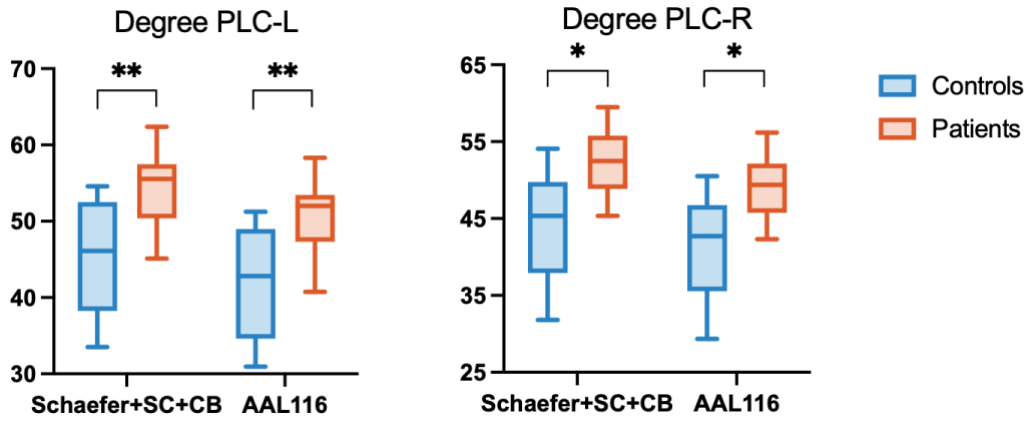

Figure 3: Local graph metrics that show significant differences between patients (M) and controls (HC) for both parcellations. The boxplots represent distributions of the metrics across subjects. Significant differences between groups are indicated (*p<0.05, **p<0.01). The node degree of the right and left Posterior Lobes of the Cerebellum (PLC) is increased in migraine patients relative to healthy controls (M>HC).

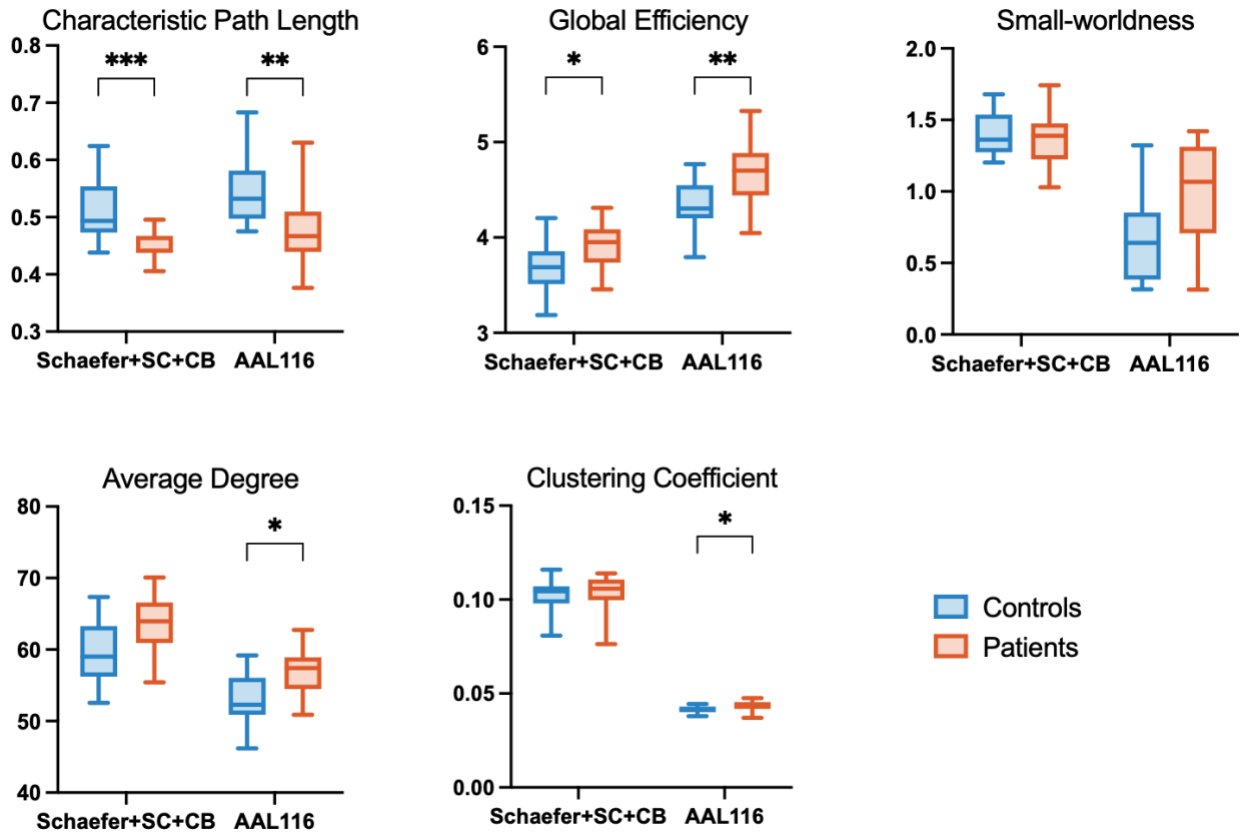

Figure 4: Global graph metrics in both patients (M) and controls (HC) for both parcellations. The boxplots represent distributions across subjects. Significant differences between groups are indicated (*p<0.05, **p<0.01, ***p<0.001). The characteristic path length is decreased in patients in both parcellations, whilst the global efficiency is increased. For the AAL116 parcellation, the average degree and the clustering coefficient are increased in patients.

Moreover, a significant positive correlation (Pearson correlation r=0.56, p=0.038) was found between the characteristic path length obtained using the Schaefer + SC + CB parcellation in patients and their disease duration (Figure 5). No other significant correlations between graph metrics and clinical parameters were found.

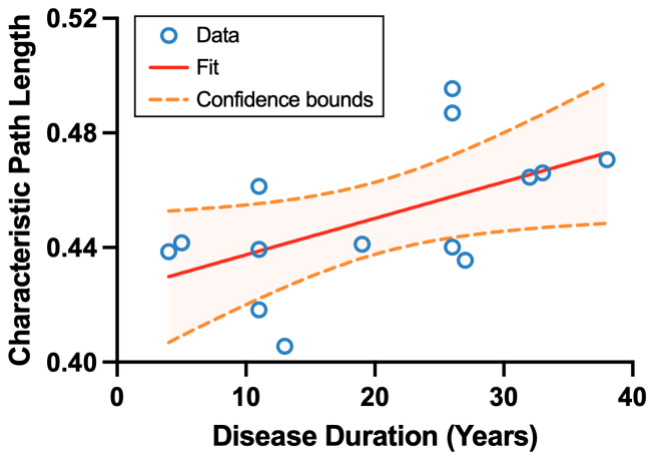

Figure 5: Correlation between the characteristic path length (from the connectome obtained with the Schaefer + SC + CB parcellation) and the disease duration for the migraine patients (Pearson correlation r=0.56 with p=0.038).

3.3. White matter tract analysis

Regarding the change in the number of reconstructed white matter streamlines, we found a significant bilateral increase in the anterior limb of the internal capsule (ALIC) in the patient group relative to controls (p=0.029 for the right ALIC and p=0.046 for the left ALIC), as shown in Figure 6.

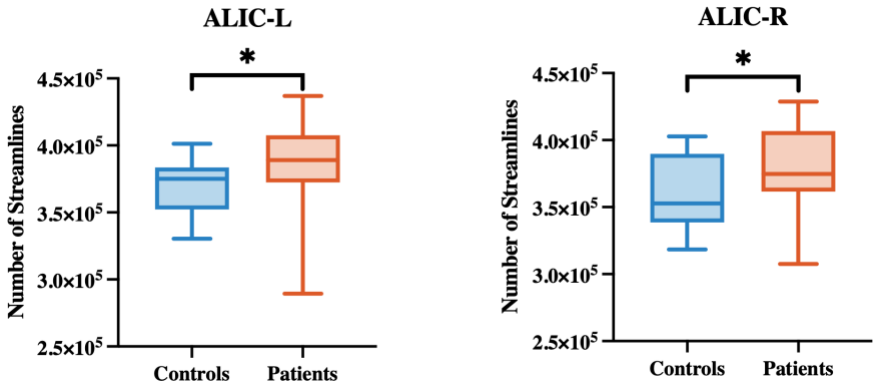

Figure 6: Number of reconstructed streamlines in the left and right anterior limb of the internal capsule (ALIC) (from the ICBM-DTI-81 white-matter labels atlas) for patients (M) and controls (HC). The boxplots represent distributions of the metrics across subjects. Significant differences between groups are indicated (*p<0.05). In both ROIs, there is an increased number of streamlines in patients.

4. DISCUSSION

In this study, the structural connectome of a group of migraine patients with episodic migraine without aura was studied using dMRI and tractography considering two different whole-brain parcellations. This is the first study, to our knowledge, to perform a connectomics analysis through tractography in migraine based on atlases that included cortical as well as subcortical, and cerebellar regions. We identified increased connectivity of cerebellar regions in migraine patients, which was reflected in the increased node degree of the posterior lobe of the cerebellum. Consistently with such increased connectivity, we also find an increased number of streamlines in the anterior limb of the internal capsule.

From a global connectome perspective, we found increased global efficiency and decreased characteristic path length in patients, which was correlated with the disease duration. This could lead to a dysfunctional modulation of the brain network in migraine and a faster dissemination of pain-related information (6). Additionally, some studies have also reported correlations between graph theory metrics or diffusion metrics and patients' clinical data. For instance, Dai et al. (7) reported a correlation between local efficiency and the visual analog scale in episodic migraine without aura, while Planchuelo-Gómez et al. (4) and Chong et al. (10) reported a relationship between diffusion metrics such as fractional anisotropy (FA) and mean diffusivity and the years lived with migraine (disease duration), using less homogeneous cohorts than ours.

Connectivity analysis

The overall patterns of increased connectivity in patients relative to controls were characterized by a strong involvement of cerebellar regions, namely the crus, the posterior lobe of the cerebellum, and the vermis.

The connectivity analysis showed increased connectivity between the crus and the posterior lobe of the cerebellum. It is believed that the crus exhibits increased activity in response to painful stimuli and has cognitive and emotional representations (28). Since the crus and the posterior lobe of the cerebellum are involved in cognitive processes (29), alterations in their connectivity may be associated with cognitive impairments frequently reported by migraine patients. In addition, stimulation of the posterior lobe of the

cerebellum has been shown to modulate the response to noxious visceral stimuli in mice (30), which could be related to migraine pathology.

We also found increased connectivity between the vermis and other regions. The posterior vermis is the anatomical substrate of the limbic cerebellum (29) and thus a disruption in the cerebro-cerebellar-limbic loops of cerebellar input could be indicative of the emergence of emotional disturbances like mood changes often observed in migraine patients.

The cerebellum has an inhibitory role in pain processing (31), having several connections to the prefrontal cortex (via the thalamus) (32). Therefore, the increased connectivity between the cerebellum and other regions could be indicative of a dysfunctional negative feedback loop in which the thalamus is not sensing the inhibitory signal (31). These connectivity results could be indicative of the importance of the cerebellum in the modulation of migraine possibly through the modulation of calcitonin gene-related peptide (CGRP) (11, 14). CGRP modulates nociception and assists in the onset of migraine, and thus it might play a role in reshaping connectivity and stabilizing synapses in the cerebellar circuitry (33, 34).

Our results not only contribute further evidence that the cerebellum plays a central role in migraine pathophysiology but also emphasize the importance of including it as a region of interest in connectome studies of migraine, with the robustness of our analysis being supported by the observation of similar patterns across two different brain parcellations.

Graph metrics analysis

At the global connectome level, decreased characteristic path length and increased global efficiency were found in patients compared to controls, which can be associated with more effective pain information propagation in the brain (3, 6, 7). Moreover, the positive correlation found between the diminished characteristic path length of patients and their disease duration (years lived with migraine) could potentially imply a plastic adaptation to migraine over time, which has been reported by several diffusion tensor imaging studies (4, 10, 35, 36) in migraine patients.

In terms of local graph metrics, we found a bilateral increase in the node degree of the posterior lobe of the cerebellum, which is consistent with the increased connectivity of this region with the rest of the brain.

White matter tract analysis

Complementarily to the analysis of the structural connections between gray matter regions, the corresponding white matter tracts were also evaluated considering the number of streamlines that passed through each tract and found a greater number of streamlines bilaterally in the anterior limb of the internal capsule of patients. The internal capsule contains ascending and descending axons including fibers to and from the thalamus, and to and from the cerebellum (37). This increase is therefore consistent with the increased connectivity of the cerebellum, and could also be indicative of the dysfunctional negative feedback loop mentioned before. On the other hand, the increased number of reconstructed fibers could also be a consequence of an increased FA in the cerebellum of patients, which other researchers (38) have found. Future studies should clarify these different possible reasons.

Limitations

This study has a few limitations, the main one being the small sample size. Despite that, we focused on a homogeneous patient group with controlled conditions and selected a well-matched control group in terms of gender, age, and menstrual cycle phase, minimizing individual variability. Furthermore, our connectivity measures are based on the number of reconstructed streamlines obtained by using a specific tractography algorithm. Although the methodology we chose is well-established and commonly used in the literature, there is no validation in place concerning ground truth data (39, 40).

5. CONCLUSION

In conclusion, our findings reveal noteworthy structural connectome alterations within a uniform cohort of patients diagnosed with episodic migraine without aura, prominently implicating the cerebellum. These results substantiate the notion of

heightened integration across whole brain networks underscoring the previously acknowledged yet often overlooked role of the cerebellum in migraine pathophysiology.

References

1. Hoffmann J, Baca SM, Akerman S. Neurovascular mechanisms of migraine and cluster headache. J Cereb Blood Flow Metab 2019; 39:573–594.

2. Ashina, Sait, et al. Structural and functional brain changes in migraine. Pain and Therapy 2021; 10: 211-223.

3. Silvestro M, Tessitore A, Caiazzo G, et al. Disconnectome of the migraine brain: a “connectopathy” model. Journal of Headache and Pain 2021; 22:1–11.

4. Planchuelo-Gómez Á, García-Azorín D, Guerrero ÁL, Aja-Fernández S, Rodríguez M, de Luis-García R. Structural connectivity alterations in chronic and episodic migraine: A diffusion magnetic resonance imaging connectomics study. Cephalalgia 2020; 40.

5. Planchuelo-Gómez Á, García-Azorín D, Guerrero ÁL, Aja-Fernández S, Rodríguez M, de Luis-García R. Multimodal fusion analysis of structural connectivity and gray matter morphology in migraine. Human Brain Mapping 2021; 42.

6. Li K, Liu L, Yin Q, et al. Abnormal rich club organization and impaired correlation between structural and functional connectivity in migraine sufferers. Brain Imaging and Behavior 2017; 11.

7. Dai L, Zheng Q, Chen X, et al. Altered brain structural topological properties and its correlations with clinical characteristics in episodic migraine without aura. Neuroradiology 2021; 63:2099–2109.

8. Liu J, Ma S, Mu J, et al. Integration of white matter network is associated with interindividual differences in psychologically mediated placebo response in migraine patients. Human Brain Mapping 2017; 38:5250–5259.

9. Michels L, Koirala N, Groppa S, et al. Structural brain network characteristics in patients with episodic and chronic migraine. J Headache Pain 2021, 22:1–13.

10. Chong CD, Schwedt TJ. Migraine affects white-matter tract integrity: A diffusion-tensor imaging study. Cephalalgia 2015; 35:1162–1171.

11. Mehnert J, May A. Functional and structural alterations in the migraine cerebellum. Journal of Cerebral Blood Flow and Metabolism 2019; 39:730–739.

12. Qin Z, He X-W, Zhang J, et al. Structural changes of cerebellum and brainstem in migraine without aura. J Headache Pain 2019; 20:93.

13. Koppen H, Boele HJ, Palm-Meinders IH, et al. 2017. Cerebellar function and ischemic brain lesions in migraine patients from the general population. Cephalalgia, 2017; 37(2), 177-190.
14. Wang M, Tutt JO, Dorricott NO, Parker KL, Russo AF, Sowers LP. Involvement of the cerebellum in migraine. Frontiers in Systems Neuroscience 2022; 16.
15. Olesen J. Headache Classification Committee of the International Headache Society (IHS) The International Classification of Headache Disorders, 3rd edition. Cephalalgia 2018; 38:1–211.
16. M.W. Woolrich, S. Jbabdi, B. Patenaude, M. Chappell, S. Makni, T. Behrens, C. Beckmann, M. Jenkinson, S.M. Smith. Bayesian analysis of neuroimaging data in FSL. NeuroImage, 45:S173-86, 2009
17. Tournier JD, Smith R, Raffelt D, et al. MRtrix3: A fast, flexible and open software framework for medical image processing and visualization. NeuroImage 2019; 202.
18. Ades-Aron B, Veraart J, Kochunov P, et al. Evaluation of the accuracy and precision of the diffusion parameter EStImation with Gibbs and NoisE removal pipeline. NeuroImage 2018; 183:532–543.
19. Jeurissen B, Tournier J-D, Dhollander T, Connelly A, Sijbers J. Multi-tissue constrained spherical deconvolution for improved analysis of multi-shell diffusion MRI data. NeuroImage 2014; 103:411–426.
20. Smith RE, Tournier J-D, Calamante F, Connelly A. Anatomically-constrained tractography: improved diffusion MRI streamlines tractography through effective use of anatomical information. Neuroimage 2012; 62:1924–1938.
21. Smith RE, Tournier J-D, Calamante F, Connelly A. SIFT2: Enabling dense quantitative assessment of brain white matter connectivity using streamlines tractography. Neuroimage 2015; 119:338–351.
22. Schaefer A, Kong R, Gordon EM, et al. Local-Global Parcellation of the Human Cerebral Cortex from Intrinsic Functional Connectivity MRI. Cerebral Cortex 2018; 28:3095–3114.
23. Tzourio-Mazoyer N, Landeau B, Papathanassiou D, et al. Automated Anatomical Labeling of Activations in SPM Using a Macroscopic Anatomical Parcellation of the MNI MRI Single-Subject Brain. NeuroImage 2002; 15:273–289.

24. Zalesky A, Fornito A, Bullmore ET. Network-based statistic: Identifying differences in brain networks. NeuroImage 2010; 53:1197–1207.
25. Yeo BTT, Krienen FM, Chee MWL, Buckner RL. Estimates of segregation and overlap of functional connectivity networks in the human cerebral cortex. NeuroImage 2014; 88:212–227.
26. Rubinov M, Sporns O. Complex network measures of brain connectivity: Uses and interpretations. NeuroImage 2010; 52:1059–1069.
27. Hua K, Zhang J, Wakana S, et al. Tract Probability Maps in Stereotaxic Spaces: Analyses of White Matter Anatomy and Tract-Specific Quantification. NeuroImage 2008; 39:336.
28. Moulton EA, Elman I, Pendse G, Schmahmann J, Becerra L, Borsook D. Aversion-Related Circuitry in the Cerebellum: Responses to Noxious Heat and Unpleasant Images. J Neurosci 2011; 31:3795–3804.
29. Stoodley CJ, Schmahmann JD. Evidence for topographic organization in the cerebellum of motor control versus cognitive and affective processing. Cortex 2010; 46:831–844.
30. Saab C, and Willis W. Nociceptive visceral stimulation modulates the activity of cerebellar Purkinje cells. Experimental brain research 2001; 140:122-126.
31. Younis S, Hougaard A, Noseda R, Ashina M. Current understanding of thalamic structure and function in migraine. Cephalalgia 2019; 39:1675–1682.
32. Middleton FA, Strick PL. Cerebellar Projections to the Prefrontal Cortex of the Primate. J Neurosci 2001; 21:700–712.
33. Morara S, Rosina A, Provini L. CGRP as a Marker of the Climbing Fibers during the Development of the Cerebellum in the Rat. Annals of the New York Academy of Sciences 1992; 657:461–463.
34. Morara S, Sternini C, Provini L, Rosina A. Developmentally regulated expression of α- and β-calcitonin gene-related peptide mRNA and calcitonin gene-related peptide immunoreactivity in the rat inferior olive. J of Comparative Neurology 1995; 354:27–38.
35. Szabó N, Faragó P, Király A, et al. Evidence for Plastic Processes in Migraine with Aura: A Diffusion Weighted MRI Study. Frontiers in Neuroanatomy 2018; 11:138.

36. Schmitz, N., Admiraal-Behloul, F., Arkink, E.B., et al. Attack Frequency and Disease Duration as Indicators for Brain Damage in Migraine. Headache: The Journal of Head and Face Pain 2008; 48: 1044-1055.
37. Waxman SG. Clinical Neuroanatomy. McGraw-Hill Medical; 2017.
38. Marciszewski KK, Meylakh N, Di Pietro F, Macefield VG, Macey PM, Henderson LA. Fluctuating Regional Brainstem Diffusion Imaging Measures of Microstructure across the Migraine Cycle. eNeuro 2019; 6:ENEURO.0005-19.2019.
39. Calamante F. The Seven Deadly Sins of Measuring Brain Structural Connectivity Using Diffusion MRI Streamlines Fibre-Tracking. Diagnostics 2019, Vol 9, Page 115 2019; 9:115.
40. Lim JC, Phal PM, Desmond PM, et al. Probabilistic MRI Tractography of the Optic Radiation Using Constrained Spherical Deconvolution: A Feasibility Study. PLoS One 2015; 10:e0118948.

Data accessibility statement

Although the data used in this study cannot be made publicly available, the implemented code can be accessed in the following repository: https://github.com/anamatoso/connectivity-analysis-diffusion

Grant support

This work was supported by the Portuguese Science Foundation through grants 2023.03810.BDANA, SFRH/BD/139561/2018, COVID/BD/153268/2023, PTDC/EMD-EMD/29675/2017, LISBOA-01-0145-FEDER-029675. This work was also supported by LARSyS funding (DOI: 10.54499/LA/P/0083/2020, 10.54499/UIDP/50009/2020, and 10.54499/UIDB/50009/2020)

Acknowledgments

We acknowledge the Portuguese Science Foundation and LARSyS for supporting our study. We also express our gratitude to the participants of this study as well as the collaborators from Hospital da Luz Lisboa.